

Adaptive memory distortions are predicted by
feature representations in parietal cortex

Yufei Zhao (赵雨菲)¹, Avi J. H. Chanales², & Brice A. Kuhl¹

Department of Psychology, University of Oregon¹, 97401

Department of Psychology, New York University², 10016

1

Abbreviated title: Memory distortions in parietal cortex

Corresponding author email address: Yufei Zhao (yzhao17@uoregon.edu) or Brice Kuhl

10 bkuhl@uoregon.edu

11 Pages: 35

12 Figures: 4

13 Tables: 1

14 **Number of words:** Abstract (152), Introduction (696), discussion (1448)

15

16 **Acknowledgements:** This work was supported by NIH grant NINDS R01-NS107727 and NSF CAREER

17 Award BCS-1752921 to B.A.K.

18

19

20

21

22

23

¹ The authors declare no competing financial interests.

25 **ABSTRACT**

26

27 Similarity between memories is a primary cause of interference and forgetting. Exaggerating subtle
28 differences between memories is therefore a potential mechanism for reducing interference. Here, we
29 report a human fMRI study ($n = 29$, 19 female) that tested whether behavioral and neural expressions of
30 memories are adaptively distorted to reduce interference. Participants learned and repeatedly retrieved
31 object images, some of which were identical except for subtle color differences. Behavioral measures of
32 color memory revealed exaggeration of differences between similar objects. Importantly, greater memory
33 exaggeration was associated with lower memory interference. fMRI pattern analyses revealed that color
34 information in parietal cortex was stronger during memory recall when color information was critical for
35 discriminating competing memories. Moreover, greater representational distance between competing
36 memories in parietal cortex predicted greater color memory exaggeration and lower memory interference.
37 Together, these findings reveal that competition between memories induces adaptive, feature-specific
38 distortions in parietal representations and corresponding behavioral expressions.

39

40 **Keywords:** episodic memory, interference, repulsion, fMRI, pattern similarity

41

42 **Significance Statement (120 words)**

43

44 Similarity between memories is a primary cause of interference and forgetting. Here, we show that when
45 remembering highly similar objects, subtle differences in the features of these objects are exaggerated in
46 memory in order to reduce interference. These memory distortions are reflected in, and predicted by,
47 overlap of activity patterns in lateral parietal cortex. These findings provide unique insight into how memory
48 interference is resolved and specifically implicate lateral parietal cortex in representing feature-specific
49 memory distortions.

50 **INTRODUCTION**

51

52 Given the vast number of memories that humans store, overlap between memories is inevitable. For
53 example, one may have taken multiple vacations to the same town or parked in the same garage on many
54 occasions. There is a long history of behavioral studies in psychology documenting the many contexts in
55 which this type of overlap leads to memory interference and forgetting (Anderson & Spellman, 1995; Barnes
56 & Underwood, 1959; Mensink & Raaijmakers, 1988; Osgood, 1949; Wixted, 2004). As a result, a primary
57 focus of theoretical models of memory has been to specify the computational mechanisms by which
58 interference is resolved (Colgin, Moser, & Moser, 2008; O'Reilly & McClelland, 1994; Treves & Rolls, 1994).
59 These models have largely focused on how memories are encoded so that the content of memories is
60 protected against interference. An alternative perspective, however, is that instead of protecting memories
61 from interference, there is adaptive value in allowing the content of memories to be *shaped* by interference
62 (Hulbert & Norman, 2015; Kim, Norman, & Turk-Browne, 2017). Specifically, to the extent that overlap
63 across memories is the root cause of interference, then distorting memories to reduce this overlap is a
64 potentially effective remedy.

65 Evidence from recent neuroimaging studies hints at the idea that memory representations are
66 distorted as an adaptive response to interference. Namely, several studies have found that when similar
67 events are encoded into memory, this triggers a targeted exaggeration of differences in patterns of activity
68 in the hippocampus (Ballard, Wagner, & McClure, 2019; Chanales, Oza, Favila, & Kuhl, 2017; Dimsdale-
69 Zucker, Ritchey, Ekstrom, Yonelinas, & Ranganath, 2018; Favila, Chanales, & Kuhl, 2016; Hulbert &
70 Norman, 2015; Kim et al., 2017; Schapiro, Kustner, & Turk-Browne, 2012; Schlichting, Mumford, & Preston,
71 2015). The key observation in these studies is that similar memories 'move apart' from each other in
72 representational space, suggesting a form of memory repulsion. Yet, a critical limitation of these studies is
73 that the feature dimensions along which memories move are underspecified. That is, do changes in neural
74 representations correspond to changes in the information content of memories? On the one hand, neural
75 activity pattern may become separated without any changes to underlying memories. Alternatively, changes
76 in neural activity patterns may reflect adaptive changes in memory content. For example, if two vacations

77 to the same city were associated with different weather conditions, then weather-related information may
78 be a salient component of corresponding memories and weather-related *differences* between those
79 vacations may be exaggerated to improve memory discriminability (e.g., “That was the year it was *really*
80 *cold*,” vs. “That was the year it was *really hot*”).

81 While it has proven difficult to translate hippocampal activity patterns to explicit feature dimensions
82 (LaRocque et al., 2013; Liang, Wagner, & Preston, 2013), feature dimensions are far more accessible in
83 (or decodable from) neocortical regions involved in memory retrieval. In particular, there is rapidly growing
84 evidence that lateral parietal cortex carries detailed information about the content of retrieved memories
85 (Chen et al., 2017; Long, Lee, & Kuhl, 2016; Xiao et al., 2017) and amplifies behaviorally-relevant
86 information (Favila, Samide, Sweigart, & Kuhl, 2018; Kuhl, Johnson, & Chun, 2013). Moreover, recent
87 studies have shown that memory representations in parietal cortex can be decomposed into separable
88 feature dimensions (Bone, Ahmad, & Buchsbaum, 2020; Favila et al., 2018; Lee, Samide, Richter, & Kuhl,
89 2019). Thus, lateral parietal cortex may provide a unique window into how memory representations are
90 shaped by interference.

91 Here, we tested whether interference between highly similar memories triggers adaptive distortions
92 in parietal memory representations and corresponding behavioral expressions of memories. Our motivating
93 theoretical perspective was that subtle differences between similar memories are prioritized and
94 exaggerated to reduce the potential for interference. To test these ideas, we modified a recent behavioral
95 paradigm that demonstrated adaptive biases in long-term memory for objects (Chanales, Tremblay-
96 McGaw, & Kuhl, in-press). We predicted that competition between memories for similar objects would
97 trigger a memory-based exaggeration of subtle differences between those objects, and that greater
98 exaggeration would be associated with lower memory interference. Using pattern-based fMRI analyses, we
99 tested whether memory representations in lateral parietal cortex (a) preferentially express features that are
100 critical for discriminating similar objects and (b) predict feature-specific distortions in behavioral expressions
101 of memory.

102

103 **Materials and Methods**

104

105 ***Participants***

106

107 Thirty-two (21 female; mean age = 23.5 years) right-handed, native English speakers from the University
108 of Oregon community participated in the experiment. Three participants were excluded from analysis (two
109 due to falling asleep inside the scanner, one due to technical error), resulting in a final set of 29 participants
110 (19 female; mean age = 23.7 years) included in data analysis. Participants were screened for motion during
111 the scanned recall tasks, but no participants exceeded the exclusion criteria (mean framewise displacement
112 > 0.25) for any of the runs. The sample size was comparable to similar fMRI studies in the field. All
113 participants had normal or corrected-to-normal vision. Informed consent was obtained in accordance with
114 the University of Oregon Institutional Review Board.

115

116 ***Overview of Experimental Paradigm***

117

118 We modified a paradigm from a recent behavioral study that was used to demonstrate adaptive biases in
119 long-term memory for object colors (Chanales, Tremblay-McGaw, & Kuhl, in-press). In the prior (and
120 current) study, participants learned associations between faces and object images. Critically, the objects
121 contained 'pirmates' for which the object images were identical except for their color (e.g., a blue backpack
122 and a purple backpack), and successful learning required discriminating between these pirmates. In the
123 current study, we used a two-day procedure in which participants received extensive behavioral training on
124 face-object associations on Day 1 and then returned on Day 2 for additional behavioral training, followed
125 by an fMRI session, and finally a behavioral color memory test (Fig. 1). A critical feature of our design is
126 that we held color similarity between pirmates constant (24 degrees apart), but we included a competitive
127 and non-competitive condition (Fig. 1b). In the competitive condition, pirmate images corresponded to the
128 *same object category* (e.g., two beanbags of slightly different colors). In the non-competitive condition,
129 pirmates corresponded to *distinct object categories* (e.g., a pillow and a ball of slightly different colors).
130 Thus, in both conditions the pirmates were 24 degrees apart in color space; but, for the competitive

131 condition, color was the only feature dimension on which the pairmates differed. In contrast, for the non-
132 competitive condition, object category also differed between pairmates. Thus, although color distance
133 between pairmates was matched across conditions, color information was more important in the competitive
134 condition. For the fMRI session, participants were shown faces, one at a time, with the only instruction
135 being to retrieve corresponding objects as vividly as possible. An important feature of our procedure is that
136 participants were not explicitly instructed to retrieve color information during the fMRI scans, nor had color
137 memory been tested at any point prior to scanning. Rather, we only tested color memory after participants
138 exited the scanner.

139

140 ***Stimuli***

141

142 Participants learned associations between 24 object images and 24 images of white male faces. The 24
143 object images corresponded to 18 distinct object categories (e.g., beanbag, hat, umbrella, balloon) and 12
144 distinct color values. Thus, some of the 24 object images were from the same object category (e.g., two
145 beanbags) or had the same color value. The object images were generated from an image set that allowed
146 for each image's color to be rotated along a 360° color wheel (Brady, Konkle, Alvarez, & Oliva, 2013). To
147 assign colors to each object, the 360° color wheel was divided into 15 evenly spaced color values (0°, 24°,
148 48°, etc.). These 15 values were arbitrarily chosen but were fixed across participants. For each participant,
149 6 consecutive color values were selected (randomly positioned among the set of 15 color values) for the
150 competitive condition. For example, color values of 48°, 72°, 96°, 120°, 144°, and 168° might be selected
151 for the competitive condition (Fig. 1b). Likewise, 6 consecutive color values were selected for the non-
152 competitive condition. The 6 values for the non-competitive condition always 'started' 48° after the
153 competitive color values 'ended.' For example, if the color values for the competitive condition spanned 48°
154 to 168°, then the color values for the non-competitive condition would be 216°, 240°, 264°, 288°, 312°, 336°
155 (Fig. 1b).

156

157 For both conditions, the 6 color values were clustered into 3 sets of consecutive color values: e.g., 48° and
158 72°, 96° and 120°, 144° and 168°. Each of these sets included a total of 4 object images (resulting in 12
159 object images for each condition). For the competitive condition, the four images in each set represented
160 two color values (e.g., 48° and 72°) and two object categories (e.g., beanbag and jacket). For example, the
161 set might include a 48° beanbag, a 72° beanbag, a 48° jacket and a 72° jacket (Fig. 1b). Object images
162 within each set that were from the same object category (e.g., the 48° beanbag and the 72° beanbag) are
163 referred to as 'pairmates.' For the non-competitive condition, the four images in each set represented two
164 color values (e.g., 216° and 240°) and four distinct object categories (Fig. 1b). Although none of the object
165 images in the non-competitive condition were from the same object category, the four images in each set
166 were also divided into pairmates, with pairmates being images from distinct object categories and, as in the
167 competitive condition, with color values 24° apart. For example, if a set in the non-competitive condition
168 included a 216° lunchbox, a 216° pillow, a 240° hat, and a 240° ball, the 216° lunchbox and the 240° hat
169 might be arbitrarily designated as one set of pairmates and the 216° pillow and the 240° ball as the other
170 set of pairmates. These non-competitive pairmates functioned as a critical control condition for behavioral
171 and fMRI analyses (see *fMRI Pattern Similarity Analyses*, below).

172

173 The mapping between the 24 object images and the 24 face images was randomly determined for each
174 participant. All face and object images were 250 * 250 pixels.

175

176 ***Pre-scan face-object training***

177

178 Participants completed the experiment on two consecutive days (Fig. 1a). On Day 1, participants learned
179 24 face-object associations across 14 training rounds. Each training round consisted of a study phase and
180 an associative memory test phase. During study phases, participants were presented with the 24 face-
181 object associations, one association at a time, in random order. Each trial started with a fixation cross
182 presented in the center of the screen (1.5 s), followed by the face-object association (3.5 s). Faces were
183 presented to the left of the objects. During the associative memory test phases, object images were

184 presented at the top of the screen with four face choices below. The four face choices always included the
185 target face (i.e., the face associated with the presented object image), the pairmate's face (i.e., the face
186 that was associated with the presented object's pairmate), and two foil faces (associated with non-pairmate
187 objects). Participants were asked to select the face that was associated with the presented object. After
188 responding, participants received feedbacks indicating whether or not they were correct and showing the
189 correct face-object association for 1.5 s. Each trial in the associative memory test was self-paced up to a
190 maximum of 8 s. On Day 2, participants completed 4 additional training rounds immediately prior to entering
191 the fMRI scanner. The procedure was the same as on Day 1.

192

193 ***Scanned perception and cued recall tasks***

194

195 During fMRI scanning, participants completed 6 consecutive rounds of a perception task and 6 consecutive
196 rounds of a cued recall task (each round corresponded to a separate fMRI scan). The order of the
197 perception and cued recall tasks was counterbalanced across participants. In the perception task, each trial
198 presented one of the 24 object images in the center of the screen for 0.5 s followed by a fixation cross for
199 3.5 s. A black cross was embedded within the object images at a random location on 25% of trials and
200 participants were instructed to make a button press whenever they detected a black cross. In each
201 perception round, each object image was presented twice, in block randomized order. Participants were
202 instructed to remain centrally-fixated, on a white fixation cross, throughout each perception run. Each
203 perception round contained a 10 s null trial (fixation cross only) at the beginning and end of each scan and
204 12 null trials (4 s each) randomly distributed throughout the run. Here, we do not consider data from the
205 perception task because (a) our primary hypotheses related to participants' *memories* for the object images
206 and (b) subtle color differences between were more to detect in the scanner environment.

207

208 In the cued recall task, each trial started with one of the 24 face images presented at the center of the
209 screen for 0.5 s, followed by a blank screen for 2.5 s, and then a question mark for 1 s. Participants were
210 instructed to recall the object image that was associated with the presented face as vividly as possible and

211 to hold the image in mind throughout the trial. Participants were instructed to rate the vividness of their
212 memories ('vivid' or 'not vivid') via a button box response when the question mark appeared. The question
213 mark was followed by a fixation cross for 2 s before next trial began. Responses were recorded during the
214 trial and during the 2 s fixation cross between trials. Together, the intertrial interval was 6 s. All face-object
215 associations were tested twice in each retrieval round, in block randomized order. Each retrieval round
216 contained a 10 s null trial (fixation cross only) at the beginning and end of each scan and 12 null trials (4 s
217 each) randomly distributed throughout the run.

218

219 ***Post-scan behavioral tests***

220

221 After participants completed the perception and cued recall tasks, they exited the scanner and completed
222 five rounds of the color memory test. During the color memory test, each trial began with one of the 24 face
223 images presented on the left side of the screen and the corresponding object image presented on the right
224 of the screen. Importantly, the object image was initially in grey scale. Participants were instructed to move
225 a cursor along a color wheel (Fig. 1a, c) to adjust the color of the object to the remembered color value.
226 Participants clicked the mouse to record their response and then moved on to the next trial. Each face-
227 object association was tested once per round and the task was self-paced. After completing the five color
228 memory test rounds, participants completed two final rounds of the associative memory test—the same
229 task they completed during the training rounds on Day 1 and just prior to fMRI scanning. The sole purpose
230 of the post-scan associative memory test was to motivate participants to maintain their effort and memory
231 accuracy throughout the fMRI session as the post-scan associative memory test was used to determine a
232 monetary bonus for participants (a fact which participants were made aware of prior to the fMRI scan).

233

234 ***Measuring color memory bias***

235

236 The post scan color memory test was used to measure participants' color memory for each object image.
237 However, rather than focusing on the accuracy of recall, we were critically interested in recall bias. Bias

238 was measured in two ways. The first measure—*mean signed distance*—was computed by first averaging
239 the responses across the 5 color memory test trials for each object image. The difference between the
240 mean response and the actual color value for a given object image reflects the color memory distance for
241 that object image. Critically, if the mean response was biased *away* from the color of the pairmate object
242 (Fig. 1c), the distance measure was positively signed; if the mean response was biased *toward* the color of
243 the pairmate object (Fig. 1c), the distance measure was negatively signed. By averaging the signed
244 distance measure across the 12 object images within each condition, the mean signed distance was
245 computed for each condition (competitive, non-competitive) and for each participant. The second
246 measure—*percentage of away responses*—was computed by ignoring the distance between participants'
247 responses and the actual color values and instead simply computing the percentage of responses that were
248 biased away from the color of the pairmate object. It is important to note that this measure was computed
249 at the trial level. Thus, for a given object image, if a participant recalled the object's color 'away from' the
250 pairmate on 4 out of the 5 test trials for that object image, the percentage of away responses *for that object*
251 *image* would be 80%. Although we did not expect (or observe) notable differences between the two
252 measures (mean signed distance and percentage of away responses), the percentage of away responses
253 addressed the concern that any observed effects for the mean signed distance measure were driven by a
254 few extreme responses.

255

256 ***fMRI data acquisition***

257

258 Imaging data were collected on a Siemens 3 T Skyra scanner at the Robert and Beverly Lewis Center for
259 NeuroImaging at the University of Oregon. Functional data were acquired using a T2*-weighted multiband
260 EPI sequence with whole-brain coverage (repetition time = 2 s, echo time = 36 ms, flip angle = 90°,
261 multiband acceleration factor = 3, inplane acceleration factor = 2, 72 slices, 1.7 × 1.7 × 1.7 mm voxels) and
262 a 32-channel head coil. Note that due to an *a priori* decision to focus on visual and parietal cortical areas,
263 we used a high-resolution protocol that fully covered visual/parietal regions but only partially covered frontal
264 cortex. Each perception scan (6 total) consisted of 130 total volumes. Each retrieval scan (6 total) consisted

265 of 190 total volumes. Oblique axial slices were aligned parallel to the plane defined by the anterior and
266 posterior commissures. A whole-brain T1-weighted MPRAGE 3D anatomical volume (1 × 1 × 1 mm voxels)
267 was also collected.

268

269 ***fMRI data preprocessing***

270

271 fMRI data preprocessing was performed using fMRIprep 1.3.1 (Esteban et al., 2019). The T1-weighted
272 (T1w) image was corrected for intensity non-uniformity with N4BiasFieldCorrection (Tustison et al., 2010)
273 and skull-stripped using antsBrainExtraction.sh (ANTs 2.2.0) with OASIS30ANTS as the target template.
274 Brain surfaces were reconstructed using recon-all from FreeSurfer 6.0.1 (Dale, Fischl, & Sereno, 1999).
275 Spatial normalization to the ICBM 152 Nonlinear Asymmetrical template version 2009c (Fonov, Evans,
276 McKinstry, Almlí, & Collins, 2009) was performed through nonlinear registration with antsRegistration (ANTs
277 2.2.0). For the functional data, susceptibility distortion corrections were estimated using 3dQwarp (Cox &
278 Hyde, 1997). The BOLD reference was then co-registered to the T1w reference by bbregister (FreeSurfer)
279 using boundary-based registration with nine degrees of freedom (Greve & Fischl, 2009). Head-motion
280 parameters were estimated by mcflirt from FSL 5.0.9 (Jenkinson, Bannister, Brady, & Smith, 2002). Slice-
281 time correction was done by 3dTshift from AFNI 20160207 (Cox & Hyde, 1997). Functional data were
282 smoothed with a 1.7 mm FWHM Gaussian kernel and high pass filtered at 0.01Hz. Smoothing and filtering
283 were done with the Nipype pipeline tool (Gorgolewski et al., 2011).

284

285 Response estimates were obtained for each trial (one regressor per trial, 4 s duration) in each cued recall
286 run using the “least-squares separate” method (Mumford, Turner, Ashby, & Poldrack, 2012). With this
287 method, each item was estimated in a separate GLM as a separate regressor while all remaining items
288 were modeled together with another regressor. The six movement parameters and framewise displacement
289 were included in each GLM as confound regressors. This resulted in *t* maps that were used for the pattern
290 similarity analysis. Given that all analyses averaged data across multiple trials—mitigating the influence of
291 any one trial—we did not perform any data exclusion for outliers at the trial level.

292

293 ***Regions of interest***

294

295 fMRI analyses were conducted using a set of visual and parietal regions of interest (ROIs) that were
296 identical to those used by Favila, Samide, Sweigart, & Kuhl (2018) to measure object and color
297 representations during memory recall. While our primary focus was on the parietal ROIs, we anticipated
298 that visual regions might also reflect feature-specific information during memory retrieval. For low level
299 visual regions, we combined bilateral V1v and V1d as V1 and combined bilateral LO1 and LO2 as LO based
300 on Wang, Mruczek, Arcaro, & Kastner (2014). For high level visual regions, we generated a VTC ROI by
301 combining bilateral fusiform gyrus, collateral sulcus, and lateral occipitotemporal sulcus derived from the
302 output of Freesurfer segmentation routines. For lateral parietal cortex, we referenced Yeo et al. (2011)'s
303 17-network resting state atlas. The parietal nodes from Network 12 and 13 (subcomponents of the
304 frontoparietal control network) are referred to as dorsal lateral intraparietal sulcus (dLatIPS) and ventral
305 lateral intraparietal sulcus (vLatIPS), respectively. For the parietal node of Network 5 (dorsal attention
306 network), we separated it along the intraparietal sulcus to create a dorsal region we refer to as posterior
307 intraparietal sulcus (pIPS) and a ventral region we refer to as ventral IPS (vIPS) (Sestieri et al., 2017) . The
308 vertices in lateral occipital cortex were eliminated in these two regions. The parietal nodes of Networks 15–
309 17 (subcomponents of the default mode network) were combined into a region we refer to as angular gyrus
310 (AnG).

311

312 For post hoc analyses, we generated medial temporal and hippocampus subfield ROIs using ASHS
313 (Yushkevich et al., 2015). We selected bilateral CA1, subiculum, entorhinal cortex, and parahippocampal
314 cortex. We combined CA2, CA3 and dentate gyrus into a single ROI (CA23DG) and combined BA35 and
315 BA36 into a perirhinal cortex ROI.

316

317 ***fMRI Pattern similarity analyses***

318

319 Pattern similarity analyses were used to measure the similarity of fMRI activity patterns for various pairs of
320 object images during the cued recall task. To calculate pattern similarity, we first computed the mean activity
321 pattern for each of the 24 recalled objects by averaging t maps for odd runs and even runs separately.
322 Pearson correlations were then computed between the mean t map of odd runs and even runs. All the
323 correlations were z -transformed (Fisher's z) before subsequent analyses. All analyses were performed in
324 the participant's native T1w space and were done separately for each ROI. Pattern similarity analyses
325 focused on three specific correlations within each 'set' of 4 object images (see Fig. 1b and *Stimuli* for
326 explanation of 'sets'): (1) 'Pairmate correlations' (see *Stimuli* for definition of pairmates), (2) 'Same-color
327 correlations,' which refer to correlations between object images from different object categories but with
328 identical color values (Fig. 1b), and (3) 'Baseline correlations,' which refer to object images from different
329 object categories and different color values (24 degrees apart; Fig 1b). Again, it is important to emphasize
330 that all pattern similarity analyses were performed within the sets of 4 object images and, critically, the same
331 correlations were applied for the competitive and non-competitive conditions.

332

333 ***Neural representation of color information***

334

335 To test whether representation of color information was stronger in the competitive condition than the non-
336 competitive condition, we first obtained (for each condition, ROI, and participant) the mean 'Same-color
337 correlation' and the mean 'Baseline correlation.' Both of these correlations reflect correlations between
338 object images from different object categories (Fig. 1b), but the same-color correlation reflects images with
339 identical color values whereas the baseline correlation reflects images with a 24° difference in color. Thus,
340 the difference between these measures (same-color – baseline) isolates color-related similarity. Of critical
341 interest was whether this color-related similarity was stronger in the competitive condition than the non-
342 competitive condition. Critically, color similarity was *objectively identical* across conditions, but we predicted
343 stronger color representation in the competitive condition owing to its greater diagnostic value in the
344 competitive condition. It is important to note that the inclusion of a separate baseline correlation for each
345 condition (competitive, non-competitive) controlled for potential global similarity differences between

346 conditions (i.e., that correlations among *all pairs* of object images might be higher in one condition vs. the
347 other).

348

349 ***Neural similarity between pairmates***

350

351 To test whether similarity between pairmates was stronger in the competitive condition than the non-
352 competitive condition, we first obtained (for each condition, ROI, and participant) the mean ‘Pairmate
353 correlation’ and the mean ‘Baseline correlation.’ For the competitive condition, pairmate correlations reflect
354 object images from the same object category but with a 24° difference in color (Fig. 1b). For the non-
355 competitive condition, pairmate correlations reflect object images from different object categories, again
356 with a 24° difference in color (Fig. 1b). Thus, pairmate similarity was *objectively greater* in the competitive
357 condition than the non-competitive condition. For both conditions, the baseline correlations reflect object
358 images from different object categories and with a 24° difference in color. Thus, the difference between
359 these measures (pairmate – baseline) was intended to isolate object-related similarity (specifically for the
360 competitive condition). As with the color information analysis, the condition-specific baseline correlations
361 controlled for potential global similarity differences between conditions.

362

363 ***Neural measures of pairmate similarity predict color memory repulsion***

364

365 To test whether similarity between vIPS representations of pairmates during competitive recall predicted
366 the degree to which there was repulsion of color memories (as measured in the post-scan color memory
367 test), we first computed the mean signed color memory distance for the two objects in each set of pairmates.
368 This yielded a single value representing the distance between a given set of pairmates, with greater
369 distance reflecting greater repulsion. Next, for vIPS we computed *dissimilarity* between each set of
370 pairmates, as defined by: 1 – the Pairmate correlation. (Note: for this analysis we used dissimilarity, as
371 opposed to similarity, simply for ease of interpretation). Thus, for each participant and for each condition
372 (competitive, non-competitive), this resulted in 6 values representing color memory distance between each

373 set of pairmates and 6 values representing vIPS dissimilarity between each set of pairmates. We then
374 performed a Spearman correlation between these two measures. For each condition, one-sample *t*-tests
375 were performed on the participants' *z*-transformed Spearman's r_s values to test whether the mean
376 correlation between color memory distance and vIPS dissimilarity differed from 0. For comparison, similar
377 analyses were also performed for other ROIs (Table 1).

378

379 To better visualize the relationship between color memory distance and vIPS dissimilarity, for each
380 participant the 6 pairmates in the competitive condition were divided into three bins (2 pairmates per bin)
381 based on vIPS pairmate dissimilarity (low, medium, high). We then computed the mean signed color
382 memory distance (from the post-scan color memory test) and the mean associative memory accuracy (from
383 the pre-scan associative memory test) for each of these bins. One-way ANOVA was used to test whether
384 mean signed distance and/or mean associative memory accuracy varied as a function of vIPS dissimilarity
385 bin. Finally, we performed a multilevel mediation analysis to test whether color memory mediated the
386 relationship between vIPS pairmate dissimilarity and associative memory accuracy. This analysis was
387 performed by obtaining, for each participant, the mean color memory distance, vIPS dissimilarity, and
388 associative memory performance for each of the 6 pairmates in each condition. Mediation analyses
389 included a random intercept for each participant, but random slopes were not included due to the small
390 number of data points per condition/participant.

391

392 **Statistical analysis**

393

394 Statistical analyses were performed using R version 3.6.3. All *t*-tests were two-tailed, with $\alpha = 0.05$. All
395 repeated measures ANOVAs were computed with the afex package using Type III sums of squares. Effect
396 sizes for *t*-tests were estimated using the effsize package. Multilevel mediation analyses were computed
397 using the mediation package. Multilevel models were built using the lme4 package. All error bars in the
398 figures represent S.E.M.

399

400 **RESULTS**

401

402 ***Associative Memory Performance***

403

404 Participants completed three separate sessions that tested memory for object-face associations (14 rounds
405 on Day 1; 4 rounds before scanning on Day 2; 2 rounds after scanning on Day 2; Fig. 1a). Participants
406 showed improved accuracy across test rounds in the Day 1 session, from a mean of 56.9% ($SD = 12.8\%$)
407 on round 1 to a mean of 95.5% ($SD = 4.8\%$) on round 14 (main effect of test round: $F_{5.56, 155.73} = 91.29, p <$
408 0.0001, $\eta^2 = 0.55$). Accuracy did not vary by test round for either of the Day 2 sessions (Day 2 pre-scan:
409 $F_{2.77, 77.63} = 1.63, p = 0.194, \eta^2 = 0.01$; Day 2 post-scan: $F_{1, 28} = 0.14, p = 0.713, \eta^2 = 0.0009$). Critically,
410 accuracy was lower in the competitive condition than the non-competitive condition for each of the sessions
411 (Day 1: $F_{1, 28} = 115.89, p < 0.0001, \eta^2 = 0.29$; Day 2 pre-scan: $F_{1, 28} = 21.8, 1 p < 0.0001, \eta^2 = 0.15$; Day 2
412 post-scan: $F_{1, 28} = 22.25, p < 0.0001, \eta^2 = 0.20$; Fig. 2a). For subsequent analyses, we focused on
413 associative memory performance from the Day 2 pre-scan session (an *a priori* decision; see Methods).
414 Notably, for the Day 2 pre-scan session, lower accuracy in the competitive condition ($M = 93.2\%$, $SD =$
415 6.9%) than the non-competitive condition ($M = 98.9\%$, $SD = 2.1\%$) was driven by an increased rate of
416 selecting faces that were associated with the pairmate image (competitive condition: $M = 6.0\%$, $SD = 6.6\%$;
417 non-competitive condition: $M = 0.2\%$, $SD = 0.6\%$; $t_{28} = 4.74, p < 0.0001$, 95% CI = [0.03 0.08], Cohen's $d =$
418 1.16, paired t -test; Fig. 2a). The rate of other errors did not differ in the competitive vs. non-competitive
419 conditions (competitive: $M = 0.8\%$, $SD = 1.4\%$; non-competitive: $M = 0.98\%$, $SD = 1.6\%$; $t_{28} = -0.18, p =$
420 0.861, 95% CI = [-0.01 0.01], Cohen's $d = -0.04$, paired t -test). Thus, as intended, the competitive condition
421 specifically increased interference between pairmate images.

422

423 ***Color Memory Bias***

424

425 Immediately after the fMRI session, participants completed a color memory test. Color memory was indexed
426 in two ways: (1) using a continuous, signed measure of distance, in degrees, between the reported and

427 actual color; positive values indicate a bias *away from* the competing memory and negative values indicate
428 a bias *toward* the competing memory, and (2) using a categorical measure of the percentage of responses
429 that were biased away from the competing memory (see Methods for details of each measure). We refer
430 to these two measures as the *signed distance* and *percentage of away responses*, respectively.

431 For the competitive condition, mean signed distance was significantly greater than 0 (5.09 ± 4.69 ,
432 mean \pm SD; $t_{28} = 5.84$, $p = 0.000003$, 95% CI = [3.30 6.87], Cohen's $d = 1.08$, one-sample t -test; Fig. 2b),
433 indicating that participants' color memory was systematically biased away from the color of the pairmate.
434 In contrast, for the non-competitive condition—where the only difference was that pairmates were not from
435 the same object category—signed distance did not differ from 0 (-0.39 ± 7.08 ; $t_{28} = -0.29$, $p = 0.771$, 95%
436 CI = [-3.08 2.31], Cohen's $d = -0.05$, one-sample t -test). Signed distance was significantly greater (i.e., a
437 stronger bias away from the pairmate) in the competitive condition compared to the non-competitive
438 condition ($t_{28} = 2.90$, $p = 0.007$, 95% CI = [1.61 9.34], Cohen's $d = 0.92$, paired t -test). These data clearly
439 demonstrate that similarity between images triggered the color memory bias.

440 The pattern of data was identical when considering the percentage of away responses. Namely,
441 the percentage of away responses was significantly greater than 50% for the competitive condition ($61.4 \pm$
442 3.6%; $t_{28} = 4.49$, $p = 0.0001$, 95% CI = [56.2% 66.6%], Cohen's $d = 0.83$, one-sample t -test; Fig. 2c), but
443 not for the non-competitive condition ($46.5 \pm 14\%$; $t_{28} = -1.35$, $p = 0.189$, 95% CI = [41.2% 51.8%], Cohen's
444 $d = -0.25$, one-sample t -test). The difference between the two conditions was also significant ($t_{28} = 3.58$, p
445 = 0.001, 95% CI = [0.06 0.23], Cohen's $d = 1.08$, paired t -test). While the percentage of away responses
446 does not contain information about the magnitude of the bias in color memory, it rules out the possibility
447 that the effects observed with the signed distance measure were driven by a minority of trials with very high
448 bias.

449

450 ***Relationship between associative memory and color memory bias***

451

452 A key component of our theoretical framework is that exaggerating the color distance (in memory) between
453 similar objects plays an adaptive role in reducing memory interference. To test this idea, we correlated each

454 participant's associative memory performance (from the Day 2 pre-scan session) with their color memory
455 performance. For the competitive condition, mean associative memory performance was positively
456 correlated with mean signed distance ($r = 0.50$, $t_{26} = 2.91$, $p = 0.007$, 95% CI = [0.15 0.73], one outlier
457 excluded for associative memory performance < 3 SD below mean; Fig. 2d), consistent with the idea that
458 stronger color memory repulsion (i.e., a bias in color memory away from the pairmate) supports lower
459 associative memory interference. For the non-competitive condition, this correlation was not significant ($r =$
460 -0.31 $t_{26} = -1.63$, $p = 0.114$, 95% CI = [-0.61 0.08], one outlier excluded for signed distance > 3 SD above
461 the mean). Thus, a bias in color memory away from the pairmate was not beneficial if the pairmate was not
462 similar to (competitive with) the target. An identical pattern of data was observed when considering the
463 percentage of away responses as an index of color memory. Namely, for the competitive condition there
464 was a positive correlation between associative memory performance and the mean percentage of away
465 responses ($r = 0.42$, $t_{26} = 2.39$, $p = 0.025$, 95% CI = [0.06 0.69], one outlier excluded for associative memory
466 performance < 3 SD below mean) and no significant correlation for the non-competitive condition ($r = -0.37$,
467 $t_{27} = -2.05$, $p = 0.050$, 95% CI = [-0.65 -0.002]).

468

469 ***Neural representation of color information during recall***

470

471 The key design feature of the competitive condition was that color information was critical for discriminating
472 between pairmates. Specifically, in the competitive condition the only difference between pairmates was a
473 24-degree color difference. This contrasts with the non-competitive condition where pairmates differed in
474 color (again 24 degrees) *and* object category. Because color information was therefore more important in
475 the competitive condition, we predicted that representation of color information during the scanned recall
476 trials would be relatively stronger in the competitive condition than the non-competitive condition. Notably,
477 participants' only instruction on the recall trials was to bring each stimulus to mind as vividly as possible
478 (mean percentage of vivid responses = 95.42%, $SD = 5.43\%$). Participants were not explicitly oriented to
479 color information nor had participants' memory for color been tested in any way to that point in the
480 experiment.

481 To test for representation of color information, we computed the mean correlation of activity
482 patterns evoked during recall of non-pairmate stimuli that shared an identical color value (e.g., red bean
483 bag and red jacket; ‘same-color’ comparison, see Fig. 1b) and subtracted from this value the mean
484 correlation between non-pairmate stimuli that were 24 degrees apart in color space (e.g., red bean bag and
485 brown jacket; ‘baseline’ comparison, see Fig. 1b). Thus, the difference between these two measures (same-
486 color – baseline) provided an index of color information. We then compared this index across the
487 competitive and non-competitive trials. Critically, in terms of physical properties of the stimuli, the
488 comparison between the competitive and non-competitive trials was perfectly matched: there was no
489 objectively greater similarity between the *stimuli included in this analysis* in the competitive condition
490 compared to the non-competitive condition—there was only a difference in the importance of the
491 information.

492 For this and subsequent fMRI analyses we used a set of visual and parietal regions of interest
493 (ROIs) previously described in Favila et al. (2018) (see Methods; Fig. 3a). Critically, these ROIs were
494 previously shown to contain color and object feature representations during a memory recall task very
495 similar to the current study. The set of ROIs included three visual ROIs (V1, LO, VTC) and five lateral
496 parietal ROIs (pIPS, dLatIPS, vLatIPS, AnG, vIPS).

497 An ANOVA with factors of condition (competitive, non-competitive) and ROI (all eight ROIs)
498 revealed a significant main effect of condition, with relatively stronger color information in the competitive
499 condition than the non-competitive condition ($F_{1,28} = 5.03, p = 0.033, \eta^2 = 0.04$). Neither the main effect of
500 ROI nor the condition x ROI interaction were significant (ROI: $F_{4,55, 127.36} = 0.12, p = 0.984, \eta^2 < 0.001$;
501 condition x ROI: $F_{4,10, 114.92} = 0.78, p = 0.542, \eta^2 = 0.008$). Considering individual ROIs, only LO and vIPS
502 exhibited significantly stronger color representation in the competitive than non-competitive condition (LO:
503 $t_{28} = 2.27, p = 0.031, 95\% \text{ CI} = [0.002, 0.03]$, Cohen’s $d = 0.69$; vIPS: $t_{28} = 2.67, p = 0.012, 95\% \text{ CI} = [0.004$
504 $0.03]$, Cohen’s $d = 0.63$; paired t -tests, uncorrected; Fig 3b). Thus, as predicted, the greater relevance of
505 color information in the competitive condition resulted in stronger representation of color information during
506 recall, despite the fact that participants had not been explicitly oriented to color information in any way by
507 this point of the experiment (the critical behavioral test of color memory occurred after fMRI scanning).

508 Post-hoc analyses of medial temporal and hippocampal ROIs (see Methods) did not reveal stronger
509 color representation in the competitive than non-competitive condition for any of the ROIs ($|t|'$ s < 1.66, p 's
510 > 0.109).

511

512 ***Neural similarity between pairmates during recall***

513

514 We next tested whether neural similarity between pairmate stimuli was greater in the competitive than non-
515 competitive condition. In terms of physical stimulus properties, pairmates were, of course, more similar in
516 the competitive condition (e.g., two bean bags 24 degrees apart in color space) than in the non-competitive
517 condition (e.g., a pillow and a ball 24 degrees apart in color space). Thus, based on stimulus properties
518 alone, fMRI pattern similarity between pairmates should be greater in the competitive condition than the
519 non-competitive condition. To measure pairmate similarity we computed the mean correlation between
520 pairmate stimuli ('pairmate' comparison, see Fig. 1b) and subtracted from this value the mean correlation
521 between non-pairmate stimuli that were also 24 degrees apart in color space ('baseline' comparison, see
522 Fig. 1b). The difference between these two values (pairmate – baseline) yielded an index of pairmate
523 similarity which was then compared across the competitive and non-competitive conditions.

524 Although pairmate similarity was numerically greater in the competitive than non-competitive
525 condition across each of the eight ROIs, an ANOVA with factors of ROI and condition did not reveal a
526 significant main effect of condition ($F_{1, 28} = 2.30, p = 0.140, \eta^2 = 0.016$). The main effect of ROI and the
527 condition x ROI interaction were also not significant (ROI: $F_{4.57, 127.90} = 0.68, p = 0.626, \eta^2 = 0.006$; condition
528 x ROI: $F_{3.82, 106.85} = 0.58, p = 0.670, \eta^2 = 0.006$). However, there was a significant effect of condition,
529 corrected for multiple comparisons (Bonferroni corrected), in vIPS, with greater pattern similarity in the
530 competitive than non-competitive conditions ($t_{28} = 3.12, p = 0.004, 95\% \text{ CI} = [0.005 0.02]$, Cohen's $d = 0.70$,
531 paired t -test; Fig. 3c). Notably, as described above (Fig. 3b), vIPS also exhibited significantly stronger color
532 representation in the competitive than non-competitive condition. Moreover, vIPS also exhibited significant
533 object and color representations during a recall task in a prior study (Favila et al., 2018). Thus, across two

534 independent studies, we have consistently observed feature representations in this ROI during memory
535 recall.

536 Post-hoc analyses of medial temporal and hippocampal ROIs (see Methods) did not reveal greater
537 pairmate similarity in the competitive than non-competitive condition for any of the ROIs ($|t|$'s < 1.42, p 's >
538 0.168).

539

540 ***Neural measures of pairmate similarity predict color memory bias***

541

542 Results from the preceding analysis revealed greater similarity in vIPS representations of pairmates in the
543 competitive condition than the non-competitive condition. While this measure of neural similarity reflects
544 the greater physical similarity between pairmates in the competitive condition than the non-competitive
545 condition, the key finding from our behavioral results is that there is an adaptive benefit to *reducing* similarity
546 (in memory) between pairmates in the competitive condition. This raises the question of whether similarity
547 between vIPS representations of pairmates during competitive recall predicted the degree to which there
548 was repulsion of color memories (as measured in the post-scan color memory test). To test this, for each
549 condition (competitive, non-competitive) we correlated fMRI measures of pairmate *dissimilarity* (1 – pattern
550 similarity) with behavioral measures of mean signed color memory distance. This analysis was performed
551 within participant (i.e., at the level of individual pairmates). Given that each condition only corresponded to
552 6 pairmates per participant, Spearman rank correlation was used in order to reduce the influence of any
553 one data point. Correlation coefficients were then z -transformed, yielding a single z -transformed value for
554 each condition and participant.

555 For the competitive condition, the mean correlation between pairmate dissimilarity in vIPS during
556 recall and mean signed color memory distance was significantly positive (vIPS: $t_{28} = 3.75$, $p = 0.0008$, 95%
557 CI = [0.34 1.14], Cohen's $d = 0.70$, one-sample t -test; Fig. 4a). In other words, the more dissimilar vIPS
558 activity patterns were when recalling pairmates, the greater the color memory repulsion effect for those
559 pairmates. There was no correlation between pairmate dissimilarity in vIPS and signed color memory
560 distance for the non-competitive condition ($t_{28} = 0.78$, $p = 0.443$, 95% CI = [-0.22 0.49], Cohen's $d = 0.14$;

561 Fig. 4a) and the difference between the competitive and non-competitive conditions was significant ($t_{28} =$
562 $2.39, p = 0.024, 95\% \text{ CI} = [0.09 \ 1.12]$, Cohen's $d = 0.61$, paired t -test). Significant positive relationships
563 were also observed when pairmate dissimilarity was measured from pIPS, VTC, and vLatIPS—again, only
564 for the competitive condition (see table 1).

565 As a complementary analysis—and to better visualize the results in vIPS—we binned pairmates,
566 for each participant, based on vIPS dissimilarity (competitive condition only). We generated three bins per
567 participant: low, medium, and high pairmate dissimilarity. We then computed the mean signed color memory
568 distance for each of these bins. A one-way ANOVA revealed a significant main effect of pairmate
569 dissimilarity in vIPS on mean signed color memory distance (Fig. 4b; $F_{1.75, 48.90} = 4.95, p = 0.014, \eta^2 = 0.062$),
570 with greater dissimilarity between vIPS representations associated with greater distance in remembered
571 color values (i.e., greater repulsion). We also computed mean accuracy on the associative memory test for
572 these same vIPS dissimilarity bins in order to more directly test whether vIPS dissimilarity was associated
573 with lower interference. Indeed, we again found a significant main effect of bin ($F_{1.78, 49.87} = 4.52, p = 0.019,$
574 $\eta^2 = 0.068$), with behavioral accuracy increasing as a function of pairmate dissimilarity in vIPS. Finally, a
575 mediation analysis performed at the level of individual pairmates (see Methods) revealed that the
576 relationship between vIPS dissimilarity and associative memory accuracy was significantly mediated by
577 signed color memory distance ($\beta = 0.12, CI = [0.02 \ 0.23], p = 0.016$, 1000 bootstrapped samples),
578 consistent with the interpretation that vIPS dissimilarity reflected the degree of color memory repulsion,
579 which in turn was associated with better associative memory accuracy (lower interference).

580

581 **DISCUSSION**

582

583 Here, we show that competition between similar memories triggers biases in their neural representations
584 and corresponding behavioral expressions. Specifically, we demonstrate that subtle, diagnostic differences
585 between events were exaggerated in long-term memory and that this exaggeration reduced interference.
586 Critically, these behavioral expressions of memory distortion were predicted by adaptive, feature-specific
587 changes to memory representations in parietal cortex.

588 Our behavioral paradigm was designed to isolate the effect that competition had on color memory.
589 Specifically, the competitive and non-competitive conditions had perfectly matched structures, with
590 equivalent color distances between pairmates in both conditions (Fig. 1b). The only difference was that
591 pairmates in the competitive condition were from the same object category. As intended, this increased the
592 number of interference-related errors, particularly during early stages of learning (Fig. 2a). The increase in
593 interference-related errors is consistent with a long history of behavioral studies of memory interference
594 (Anderson & Spellman, 1995; Mensink & Raaijmakers, 1988; Wixted, 2004). Our critical question, however,
595 was whether competition distorted memory for object *features* that were otherwise successfully
596 remembered. Results from the color memory post-test revealed a robust bias in color memory in the
597 competitive condition—that is, participants exaggerated the distance between pairmates—but no
598 systematic bias in the non-competitive condition. We refer to the bias in the competitive condition as a
599 repulsion effect in order to emphasize that the bias was triggered by the representational proximity of
600 competing memories (Bae & Luck, 2017; Chanales et al., 2017, in-press; Golomb, 2015), just as spatial
601 proximity of like-poled magnets triggers magnetic repulsion.

602 It is important to emphasize that the repulsion effect is distinct from—in fact, opposite to—an
603 interference effect. That is, interference-related errors should lead participants to occasionally recall the
604 color of the competing object—an error that would produce a bias in color memory *toward* the pairmate
605 (Fig. 1c, d). Here, we did not test color memory until the very end of the experiment, so as to avoid explicitly
606 orienting participants to color information prior to (or during) the fMRI session, but our speculation is that
607 the repulsion effect only emerged after extensive practice and as interference errors subsided (Chanales
608 et al., in-press). In this sense, the repulsion effect can be thought of as an aftereffect of initial memory
609 interference. Although repulsion reflects a form of memory error, our findings indicate that it is an adaptive
610 error: participants who exhibited a stronger repulsion effect also exhibited fewer interference-related errors
611 (Fig. 2d). To the extent that objective similarity between stimuli is a root cause of memory interference
612 (Osgood, 1949), then exaggerating the difference between stimuli in memory is a potentially powerful
613 means for reducing interference (Chanales et al., in-press; Favila et al., 2016; Hulbert & Norman, 2015).

614 Our fMRI analyses, which measured neural activity patterns as participants recalled object images,
615 provided a unique means for covertly probing the qualities of participants' memories. These analyses
616 revealed two forms of adaptive memory representations in parietal cortex. First, despite the fact that
617 participants were not instructed to think about or report objects' colors during these recall trials, we observed
618 stronger color information—across the full set of visual and parietal ROIs, and in vIPS specifically—during
619 competitive than non-competitive recall trials. The stronger representation of color information during
620 competitive trials can be viewed as an adaptive response to competition in that color information was the
621 only (or diagnostic) feature dimension for discriminating pairmates in the competitive condition.

622 Second, although pairmate similarity in vIPS was stronger during competitive than non-competitive
623 recall trials (indicating that vIPS was sensitive to object similarity; Fig. 3c), we found that greater *dissimilarity*
624 between vIPS pairmate representations during competitive recall trials was associated with greater color
625 memory repulsion and less memory interference. In other words, minimizing the overlap of neural
626 representations of pairmates was an adaptive response to competition. This relationship was observed
627 within participants, at the level of individual pairmates, but it is important to emphasize that these measures
628 were temporally offset: vIPS pattern similarity was measured during recall trials in the scanner (with the
629 only instruction being to recall objects as vividly as possible) whereas behavioral expressions of color
630 memory were only tested after scanning was completed. This again makes the point that color information—
631 in this case the subtle *difference* in pairmate colors—was a salient component of activity patterns in vIPS
632 during competitive recall.

633 Importantly, when our two main fMRI findings are taken together, they indicate that an adaptive
634 response to competition involved an *increase* in similarity between stimuli that shared a diagnostic feature
635 value (i.e., objects of the same color) but a *decrease* in similarity between stimuli that had subtly different
636 values for a diagnostic feature (i.e., pairmates, which had slightly different colors). This indicates that
637 avoiding memory interference does not necessarily require a global reduction in similarity to all other
638 memories (LaRocque et al., 2013), but instead may be accomplished by more *targeted changes* in
639 representational structure that emphasize relevant similarities as well as important differences between
640 events that are stored in memory. Critically, this idea is distinct from—if not fundamentally incompatible

641 with—the traditional, and dominant view that interference is avoided through the orthogonalization of
642 memory representations (Colgin et al., 2008; Yassa & Stark, 2011). Specifically, whereas orthogonalization
643 emphasizes an initial encoding of new memories as independent from existing memories, our findings
644 instead emphasize that the representation of a given memory is *highly dependent* on representations of
645 other memories (Hulbert & Norman, 2015).

646 Our fMRI findings also add to a growing body of evidence that implicates parietal cortex in actively
647 representing content during memory retrieval (Kuhl & Chun, 2014; Lee & Kuhl, 2016; Lee et al., 2019; Rugg
648 & King, 2018; Sestieri, Shulman, & Corbetta, 2017). Of most direct relevance, in a recent study we found
649 that vIPS (a ventral subregion of parietal cortex) actively represents color and object category information
650 during memory recall (Favila et al., 2018). However, this prior study focused on decoding the *objective*
651 *properties* of recalled stimuli and did not test whether competition influenced or distorted these
652 representations, nor did it establish a link between vIPS representations and behavioral expressions of
653 memory. The current findings provide unique evidence that representations within this same vIPS subregion
654 reflect subtle distortions in how events are remembered that are *dissociable from the objective properties*
655 *of the event*. More generally, our findings highlight the behavioral relevance and detailed nature of memory
656 representations in parietal cortex.

657 While our findings provide strong evidence that representations in parietal cortex reflect the
658 influence that competition had on memory representations, it is not necessarily the case that parietal cortex
659 was the source of this influence. Rather, competition between memories is thought to induce targeted
660 plasticity in the hippocampus (Norman, Newman, & Detre, 2007; Ritvo, Turk-Browne, & Norman, 2019). In
661 fact, hippocampal representations have been shown to specifically exaggerate differences between highly
662 similar stimuli (Ballard et al., 2019; Chanales et al., 2017; Dimsdale-Zucker et al., 2018; Favila et al., 2016;
663 Hulbert & Norman, 2015; Schapiro et al., 2012; Schlichting et al., 2015). However, these exaggerations in
664 hippocampal activity patterns have generally been observed during memory encoding or perception
665 (Ballard et al., 2019; Chanales et al., 2017; Dimsdale-Zucker et al., 2018; Favila et al., 2016; Hulbert &
666 Norman, 2015; Schapiro et al., 2012; Schlichting et al., 2015), as opposed to memory recall, and they have

667 not been translated to explicit feature spaces. Indeed, attempts to translate hippocampal activity patterns
668 to explicit feature dimensions or categories have tended to be unsuccessful (LaRocque et al., 2013; Liang
669 et al., 2013). In post hoc analyses, we did not find any evidence that competition influenced feature
670 representations in the hippocampus or medial temporal lobe ROIs. That said, one notable aspect of our
671 study is that each object was retrieved from memory many times before fMRI scanning began. Given that
672 repeated retrieval has specifically been shown to hasten the transfer of representations to parietal cortex
673 (Brodt et al., 2018, 2016), this raises the question of whether the observed findings in parietal cortex were
674 dependent on repeated retrieval. For example, it is possible that competition induces exaggerated
675 representations that are initially expressed in the hippocampus but ultimately transformed, via retrieval, into
676 stable representations in parietal cortex (Favila, Lee, & Kuhl, 2020). While the current study cannot address
677 this question, it represents an interesting avenue for future research.

678 In summary, our findings provide unique evidence that memory-based representations in parietal
679 cortex exhibit adaptive, feature-specific changes in response to competition and that these changes in
680 parietal representations predict distortions in behavioral expressions of memory. More generally, our
681 findings provide unique evidence in support of the perspective that memory distortions are an adaptive
682 component of the memory system (Schacter, Guerin, & St. Jacques, 2011).

683 **REFERENCES**

684 Anderson, M. C., & Spellman, B. A. (1995). On the status of inhibitory mechanisms in cognition: Memory
685 retrieval as a model case. *Psychological Review*. US: American Psychological Association.
686 <https://doi.org/10.1037/0033-295X.102.1.68>

687 Bae, G. Y., & Luck, S. J. (2017). Interactions between visual working memory representations. *Attention,*
688 *Perception, and Psychophysics*, 79(8), 2376–2395. <https://doi.org/10.3758/s13414-017-1404-8>

689 Ballard, I. C., Wagner, A. D., & McClure, S. M. (2019). Hippocampal pattern separation supports
690 reinforcement learning. *Nature Communications*, 10(1), 1073. [https://doi.org/10.1038/s41467-019-08998-1](https://doi.org/10.1038/s41467-019-
691 08998-1)

692 Barnes, J. M., & Underwood, B. J. (1959). “Fate” of first-list associations in transfer theory. *Journal of*
693 *Experimental Psychology*, 58(2), 97–105. <https://doi.org/10.1037/h0047507>

694 Bone, M. B., Ahmad, F., & Buchsbaum, B. R. (2020). Feature-specific neural reactivation during episodic
695 memory. *Nature Communications*, 11(1), 1945. <https://doi.org/10.1038/s41467-020-15763-2>

696 Brady, T. F., Konkle, T., Alvarez, G. A., & Oliva, A. (2013). Real-world objects are not represented as
697 bound units: Independent forgetting of different object details from visual memory. *Journal of*
698 *Experimental Psychology: General*, 142(3), 791–808. <https://doi.org/10.1037/a0029649>

699 Brodt, S., Gais, S., Beck, J., Erb, M., Scheffler, K., & Schönauer, M. (2018). Fast track to the neocortex: A
700 memory engram in the posterior parietal cortex. *Science*, 362(6418), 1045 LP – 1048.
701 <https://doi.org/10.1126/science.aau2528>

702 Brodt, S., Pöhlchen, D., Flanagin, V. L., Glasauer, S., Gais, S., & Schönauer, M. (2016). Rapid and
703 independent memory formation in the parietal cortex. *Proceedings of the National Academy of*
704 *Sciences*, 113(46), 13251 LP – 13256. <https://doi.org/10.1073/pnas.1605719113>

705 Chanales, A. J. H., Oza, A., Favila, S. E., & Kuhl, B. A. (2017). Overlap among Spatial Memories Triggers
706 Repulsion of Hippocampal Representations. *Current Biology*, 27(15), 2307-2317.e5.
707 <https://doi.org/10.1016/j.cub.2017.06.057>

708 Chanales, A. J. H., Tremblay-McGaw, A. G., & Kuhl, B. A. (in-press). Adaptive repulsion of long-term
709 memory representations is triggered by event similarity. *Psychological Science*.

710 <https://doi.org/10.1101/2020.01.14.900381>

711 Chen, J., Leong, Y. C., Honey, C. J., Yong, C. H., Norman, K. A., & Hasson, U. (2017). Shared memories
712 reveal shared structure in neural activity across individuals. *Nature Neuroscience*, 20(1).

713 <https://doi.org/10.1038/nn.4450>

714 Colgin, L. L., Moser, E. I., & Moser, M.-B. (2008). Understanding memory through hippocampal
715 remapping. *Trends in Neurosciences*, 31(9), 469–477.
716 <https://doi.org/https://doi.org/10.1016/j.tins.2008.06.008>

717 Cox, R. W., & Hyde, J. S. (1997). Software tools for analysis and visualization of fMRI data. *NMR in
718 Biomedicine*, 10(4-5), 171–178. [https://doi.org/10.1002/\(SICI\)1099-1492\(199706/08\)10:4/5<171::AID-NBM453>3.0.CO;2-L](https://doi.org/10.1002/(SICI)1099-1492(199706/08)10:4/5<171::AID-NBM453>3.0.CO;2-L)

720 Dale, A. M., Fischl, B., & Sereno, M. I. (1999). Cortical Surface-Based Analysis: I. Segmentation and
721 Surface Reconstruction. *NeuroImage*, 9(2), 179–194.
722 <https://doi.org/https://doi.org/10.1006/nimg.1998.0395>

723 Dimsdale-Zucker, H. R., Ritchey, M., Ekstrom, A. D., Yonelinas, A. P., & Ranganath, C. (2018). CA1 and
724 CA3 differentially support spontaneous retrieval of episodic contexts within human hippocampal
725 subfields. *Nature Communications*, 9(1). <https://doi.org/10.1038/s41467-017-02752-1>

726 Esteban, O., Markiewicz, C. J., Blair, R. W., Moodie, C. A., Isik, A. I., Erramuzpe, A., ... Gorgolewski, K.
727 J. (2019). fMRIprep: a robust preprocessing pipeline for functional MRI. *Nature Methods*, 16(1),
728 111–116. <https://doi.org/10.1038/s41592-018-0235-4>

729 Favila, S. E., Chanales, A. J. H., & Kuhl, B. A. (2016). Experience-dependent hippocampal pattern
730 differentiation prevents interference during subsequent learning. *Nature Communications*, 7(1),
731 11066. <https://doi.org/10.1038/ncomms11066>

732 Favila, S. E., Lee, H., & Kuhl, B. A. (2020). Transforming the Concept of Memory Reactivation. *Trends in
733 Neurosciences*. <https://doi.org/https://doi.org/10.1016/j.tins.2020.09.006>

734 Favila, S. E., Samide, R., Sweigart, S. C., & Kuhl, B. A. (2018). Parietal representations of stimulus
735 features are amplified during memory retrieval and flexibly aligned with top-down goals. *Journal of
736 Neuroscience*, 38(36), 0564–18. <https://doi.org/10.1523/JNEUROSCI.0564-18.2018>

737 Fonov, V. S., Evans, A. C., McKinstry, R. C., Almlí, C. R., & Collins, D. L. (2009). Unbiased nonlinear
738 average age-appropriate brain templates from birth to adulthood. *NeuroImage*, 47, S102.
739 [https://doi.org/https://doi.org/10.1016/S1053-8119\(09\)70884-5](https://doi.org/https://doi.org/10.1016/S1053-8119(09)70884-5)

740 Golomb, J. D. (2015). Divided spatial attention and feature-mixing errors. *Attention, Perception, &*
741 *Psychophysics*, 77(8), 2562–2569. <https://doi.org/10.3758/s13414-015-0951-0>

742 Gorgolewski, K., Burns, C., Madison, C., Clark, D., Halchenko, Y., Waskom, M., & Ghosh, S. (2011).
743 Nipype: A Flexible, Lightweight and Extensible Neuroimaging Data Processing Framework in Python
744 . *Frontiers in Neuroinformatics* . Retrieved from
745 <https://www.frontiersin.org/article/10.3389/fninf.2011.00013>

746 Greve, D. N., & Fischl, B. (2009). Accurate and robust brain image alignment using boundary-based
747 registration. *NeuroImage*, 48(1), 63–72.
748 <https://doi.org/https://doi.org/10.1016/j.neuroimage.2009.06.060>

749 Hulbert, J. C., & Norman, K. A. (2015). Neural Differentiation Tracks Improved Recall of Competing
750 Memories Following Interleaved Study and Retrieval Practice. *Cerebral Cortex*, 25(10), 3994–4008.
751 <https://doi.org/10.1093/cercor/bhu284>

752 Jenkinson, M., Bannister, P., Brady, M., & Smith, S. (2002). Improved Optimization for the Robust and
753 Accurate Linear Registration and Motion Correction of Brain Images. *NeuroImage*, 17(2), 825–841.
754 <https://doi.org/https://doi.org/10.1006/nimg.2002.1132>

755 Kim, G., Norman, K. A., & Turk-Browne, N. B. (2017). Neural differentiation of incorrectly predicted
756 memories. *Journal of Neuroscience*, 37(8), 2022–2031.

757 Kuhl, B. A., & Chun, M. M. (2014). Successful Remembering Elicits Event-Specific Activity Patterns in
758 Lateral Parietal Cortex. *Journal of Neuroscience*, 34(23), 8051–8060.
759 <https://doi.org/10.1523/jneurosci.4328-13.2014>

760 Kuhl, B. A., Johnson, M. K., & Chun, M. M. (2013). Dissociable Neural Mechanisms for Goal-Directed
761 Versus Incidental Memory Reactivation. *Journal of Neuroscience*, 33(41), 16099–16109.
762 <https://doi.org/10.1523/jneurosci.0207-13.2013>

763 LaRocque, K. F., Smith, M. E., Carr, V. A., Witthoft, N., Grill-Spector, K., & Wagner, A. D. (2013). Global

764 Similarity and Pattern Separation in the Human Medial Temporal Lobe Predict Subsequent Memory.

765 *Journal of Neuroscience*, 33(13), 5466–5474. <https://doi.org/10.1523/JNEUROSCI.4293-12.2013>

766 Lee, H., & Kuhl, B. A. (2016). Reconstructing Perceived and Retrieved Faces from Activity Patterns in

767 Lateral Parietal Cortex. *Journal of Neuroscience*, 36(22), 6069–6082.

768 <https://doi.org/10.1523/JNEUROSCI.4286-15.2016>

769 Lee, H., Samide, R., Richter, F. R., & Kuhl, B. A. (2019). Decomposing Parietal Memory Reactivation to

770 Predict Consequences of Remembering. *Cerebral Cortex*, 29(8), 3305–3318.

771 <https://doi.org/10.1093/cercor/bhy200>

772 Liang, J. C., Wagner, A. D., & Preston, A. R. (2013). Content Representation in the Human Medial

773 Temporal Lobe. *Cerebral Cortex*, 23(1), 80–96. <https://doi.org/10.1093/cercor/bhr379>

774 Long, N. M., Lee, H., & Kuhl, B. A. (2016). Hippocampal Mismatch Signals Are Modulated by the Strength

775 of Neural Predictions and Their Similarity to Outcomes. *Journal of Neuroscience*, 36(50), 12677–

776 12687.

777 Mensink, G.-J., & Raaijmakers, J. G. (1988). A model for interference and forgetting. *Psychological*

778 *Review*, 95(4), 434–455. <https://doi.org/10.1037/0033-295X.95.4.434>

779 Mumford, J. A., Turner, B. O., Ashby, F. G., & Poldrack, R. A. (2012). Deconvolving BOLD activation in

780 event-related designs for multivoxel pattern classification analyses. *NeuroImage*, 59(3), 2636–2643.

781 <https://doi.org/https://doi.org/10.1016/j.neuroimage.2011.08.076>

782 Norman, K. A., Newman, E. L., & Detre, G. (2007). A Neural Network Model of Retrieval-Induced

783 Forgetting. *Psychological Review*, 114(4), 887–953. <https://doi.org/10.1037/0033-295X.114.4.887>

784 O'Reilly, R. C., & McClelland, J. L. (1994). Hippocampal conjunctive encoding, storage, and recall:

785 Avoiding a trade-off. *Hippocampus*, 4(6), 661–682. <https://doi.org/10.1002/hipo.450040605>

786 Osgood, C. E. (1949). The similarity paradox in human learning: a resolution. *Psychological Review*. US:

787 American Psychological Association. <https://doi.org/10.1037/h0057488>

788 Ritvo, V. J. H., Turk-Browne, N. B., & Norman, K. A. (2019). Nonmonotonic Plasticity: How Memory

789 Retrieval Drives Learning. *Trends in Cognitive Sciences*, 23(9), 726–742.

790 <https://doi.org/10.1016/j.tics.2019.06.007>

791 Rugg, M. D., & King, D. R. (2018). Ventral lateral parietal cortex and episodic memory retrieval. *Cortex*,
792 107, 238–250. <https://doi.org/https://doi.org/10.1016/j.cortex.2017.07.012>

793 Schacter, D. L., Guerin, S. A., & St. Jacques, P. L. (2011). Memory distortion: An adaptive perspective.
794 *Trends in Cognitive Sciences*, 15(10), 467–474. <https://doi.org/10.1016/j.tics.2011.08.004>

795 Schapiro, A. C., Kustner, L. V., & Turk-Browne, N. B. (2012). Shaping of object representations in the
796 human medial temporal lobe based on temporal regularities. *Current Biology*, 22(17), 1622–1627.
797 <https://doi.org/10.1016/j.cub.2012.06.056>

798 Schlichting, M. L., Mumford, J. A., & Preston, A. R. (2015). Learning-related representational changes
799 reveal dissociable integration and separation signatures in the hippocampus and prefrontal cortex.
800 *Nature Communications*, 6(1), 8151. <https://doi.org/10.1038/ncomms9151>

801 Sestieri, C., Shulman, G. L., & Corbetta, M. (2017). The contribution of the human posterior parietal
802 cortex to episodic memory. *Nature Reviews Neuroscience*, 18(3), 183–192.
803 <https://doi.org/10.1038/nrn.2017.6>

804 Treves, A., & Rolls, E. T. (1994). Computational analysis of the role of the hippocampus in memory.
805 *Hippocampus*, 4(3), 374–391. <https://doi.org/10.1002/hipo.450040319>

806 Tustison, N. J., Avants, B. B., Cook, P. A., Zheng, Y., Egan, A., Yushkevich, P. A., & Gee, J. C. (2010).
807 N4ITK: Improved N3 Bias Correction. *IEEE Transactions on Medical Imaging*, 29(6), 1310–1320.
808 <https://doi.org/10.1109/TMI.2010.2046908>

809 Wang, L., Mruczek, R. E. B., Arcaro, M. J., & Kastner, S. (2014). Probabilistic Maps of Visual Topography
810 in Human Cortex. *Cerebral Cortex*, 25(10), 3911–3931. <https://doi.org/10.1093/cercor/bhu277>

811 Wixted, J. T. (2004). The Psychology and Neuroscience of Forgetting. *Annual Review of Psychology*,
812 55(1), 235–269. <https://doi.org/10.1146/annurev.psych.55.090902.141555>

813 Xiao, X., Dong, Q., Gao, J., Men, W., Poldrack, R. A., & Xue, G. (2017). Transformed Neural Pattern
814 Reinforcement during Episodic Memory Retrieval. *The Journal of Neuroscience*, 37(11), 2986–2998.
815 <https://doi.org/10.1523/JNEUROSCI.2324-16.2017>

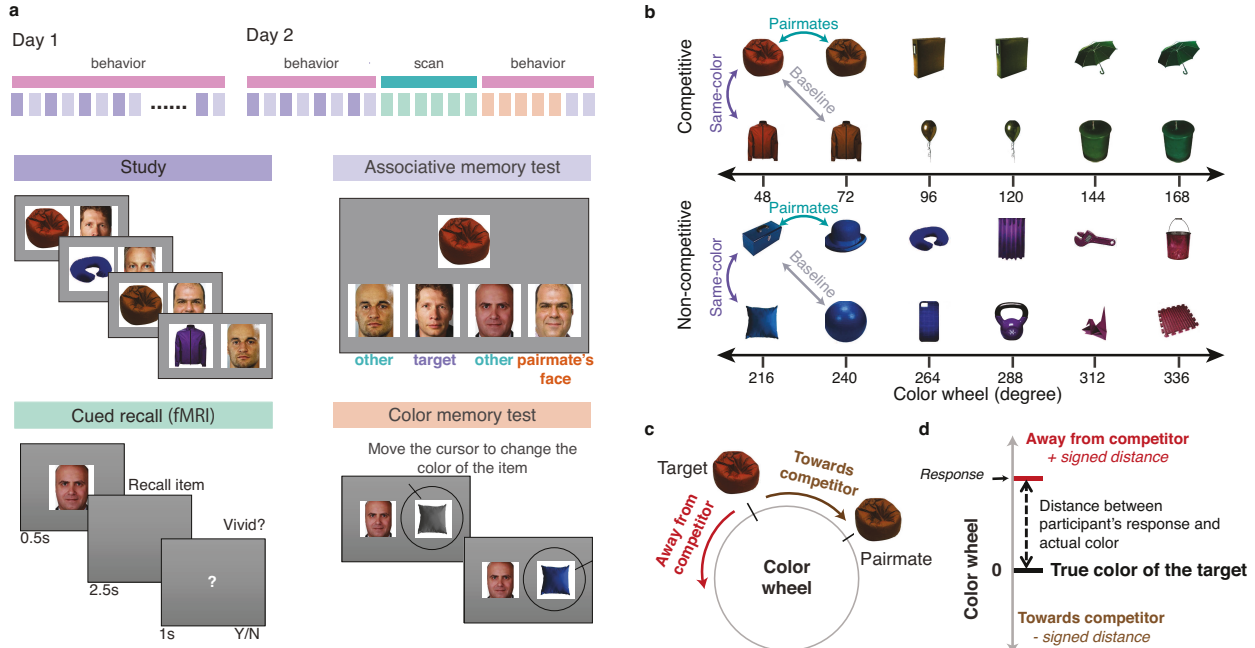
816 Yassa, M. A., & Stark, C. E. L. (2011). Pattern separation in the hippocampus. *Trends in Neurosciences*,
817 34(10), 515–525. <https://doi.org/https://doi.org/10.1016/j.tins.2011.06.006>

818 Yeo, B. T., Krienen, F. M., Sepulcre, J., Sabuncu, M. R., Lashkari, D., Hollinshead, M., ... Buckner, R. L.
819 (2011). The organization of the human cerebral cortex estimated by intrinsic functional connectivity.
820 *Journal of Neurophysiology*, 106(3), 1125–1165. <https://doi.org/10.1152/jn.00338.2011>
821 Yushkevich, P. A., Pluta, J. B., Wang, H., Xie, L., Ding, S.-L., Gertje, E. C., ... Wolk, D. A. (2015).
822 Automated volumetry and regional thickness analysis of hippocampal subfields and medial temporal
823 cortical structures in mild cognitive impairment. *Human Brain Mapping*, 36(1), 258–287.
824 <https://doi.org/10.1002/hbm.22627>
825

826 **Table 1.** Summary of key statistical analyses. Color representation analyses refer to paired-samples *t*-tests
 827 comparing color similarity effects (see Methods) for the competitive vs. non-competitive conditions.
 828 Pairmate similarity analyses refer to paired-samples *t*-tests comparing pairmate similarity effects (see
 829 Methods) for the competitive vs. non-competitive conditions. The relation to mean signed distance refers
 830 to one-sample *t*-tests comparing *z*-transformed correlations between fMRI pairmate dissimilarity and mean
 831 signed color memory distance to a test statistic of 0 (no relationship). Results from individual visual and
 832 parietal ROIs are presented in separate rows. Note: * $p < .05$, uncorrected; ** $p < .05$, Bonferroni corrected;
 833 *** $p < .01$, Bonferroni corrected.
 834

ROI	Color representation		Pairmate similarity		Relation to mean signed distance			
					Competitive		Non-competitive	
	<i>t</i> ₂₈	<i>p</i>	<i>t</i> ₂₈	<i>p</i>	<i>t</i> ₂₈	<i>p</i>	<i>t</i> ₂₈	<i>p</i>
V1	1.22	0.232	0.89	0.382	0.82	0.417	-0.34	0.734
LO	2.27	0.031*	1.71	0.098	1.34	0.190	-0.75	0.458
VTC	1.16	0.257	0.45	0.653	2.13	0.042*	0.59	0.558
pIPS	1.85	0.075	0.84	0.409	3.08	0.005**	1.08	0.289
dLatIPS	1.68	0.104	0.73	0.472	1.50	0.145	0.65	0.520
vLatIPS	1.69	0.101	0.52	0.609	2.92	0.007**	-1.89	0.069
AnG	0.57	0.573	0.36	0.720	0.75	0.462	-0.72	0.475
vIPS	2.67	0.012*	3.12	0.004**	3.75	0.0008***	0.78	0.443

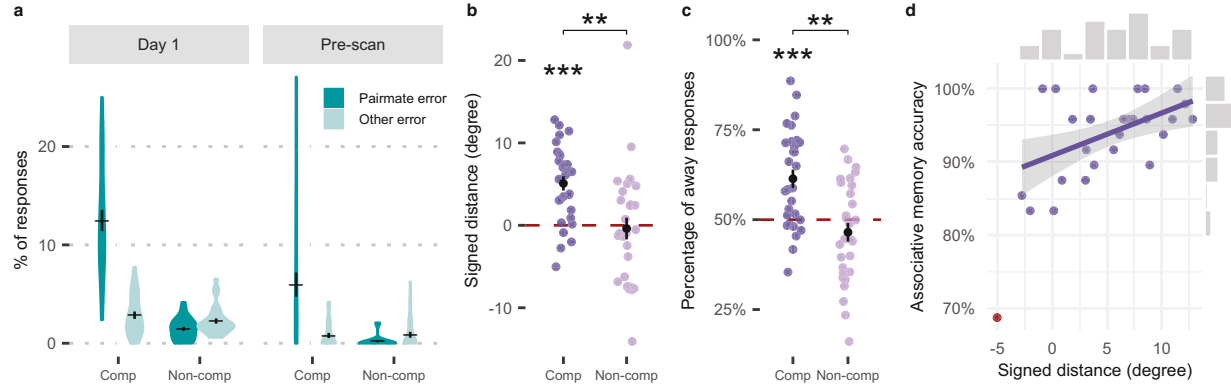
835
 836
 837
 838
 839
 840
 841
 842
 843
 844
 845



846
847
848
849
850
851
852
853
854
855
856
857
858
859
860
861
862
863
864
865
866
867
868

869

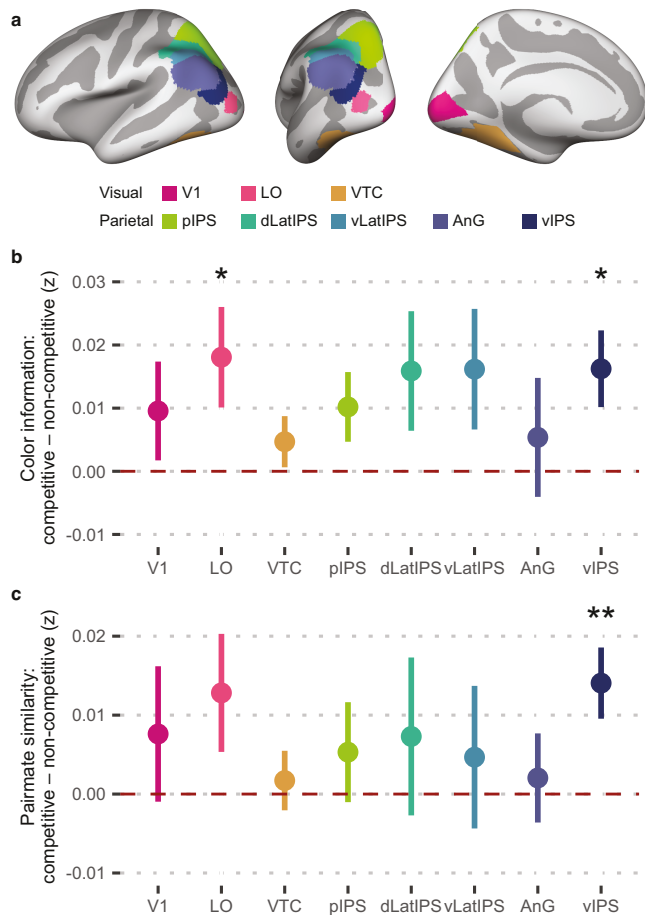
Fig. 1. Experimental Design and Procedure. **a**, Overview of paradigm. On Day 1, participants completed 14 Study and Associative Memory Test rounds. During Study, participants were shown object-face pairs and during Associative Memory Test, participants were shown an object and selected the corresponding face from a set of four choices. The set of four choices included the target face along with the face associated with the object's pairmate. On Day 2, participants completed four additional Study and Associative Memory Test rounds before entering the fMRI scanner. During scanning, participants completed a Cued Recall task during which face images were shown and participants recalled the corresponding image and indicated, by button press, the vividness of their recall. After exiting the scanner, participants completed a Color Memory Test during which a face image was shown alongside a greyscale version of the corresponding object. Participants used a continuous color wheel to indicate their memory for the object's color. Finally participants completed 2 more Associative Memory Test rounds. **b**, Sample structure of object stimuli. For both the competitive and non-competitive conditions, pairmate stimuli were 24 degrees apart in color space. For the competitive condition, pairmates were from the same object category; for the non-competitive condition, pairmates were from distinct categories. For both conditions, some objects had identical colors (Same-color). fMRI pattern similarity for Pairmate and Same-color comparisons were compared against a Baseline comparison of stimuli that were from different object categories and 24 degrees apart in color space. **c,d**, Responses on the color memory test were used to categorize memory for each object's color as being biased toward or away from the color of the competing object (**c**) and to measure the signed distance, in degrees, between participants' responses and the true color of the target (**d**).



870
871

872 **Fig. 2. Behavioral results.** a, Associative memory performance across the experiment. The overall error
873 rate (pairmate error + other error) was higher in the competitive condition than the non-competitive condition
874 for each of the associative memory test sessions (Day 1, Day 2 pre-scan, Day 2 post-scan (not shown); all
875 p 's < 0.0001). Subsequent analyses focused on associative memory performance from the Day 2 pre-scan
876 session. For the Day 2 pre-scan session, participants were significantly more likely to select faces that were
877 associated with the pairmate image (pairmate error) in the competitive condition ($M = 6.0\%$, $SD = 6.6\%$)
878 compared to the non-competitive condition ($M = 0.2\%$, $SD = 0.6\%$; $p < 0.0001$), confirming that similarity
879 between pairmates was a source of interference. b, Signed distance of responses in the color memory test.
880 For the competitive condition, mean signed distance was significantly greater than 0 ($p = 0.000003$),
881 reflecting a bias away from the color of the pairmate object (repulsion). Signed distance did not differ from
882 0 in the non-competitive condition ($p = 0.771$). The difference between the competitive and non-competitive
883 conditions was also significant ($p = 0.007$). c, Percentage of away responses in the color memory test. The
884 percentage of color memory responses 'away from' the color of the pairmate object was significantly greater
885 than 50% for the competitive condition ($p = 0.0001$), but not for the non-competitive condition ($p = 0.189$).
886 The difference between the competitive and non-competitive conditions was also significant ($p = 0.001$). d,
887 Relationship between associative memory accuracy and mean signed color memory distance. For the
888 competitive condition, participants with greater mean signed color memory distance (greater repulsion)
889 exhibited better associative memory accuracy [$r = 0.50$, $p = 0.007$, one outlier (red dot) excluded for
890 associative memory performance < 3 SD below mean]. Notes: colored dots reflect data from individual
891 participants. Error bars reflect +/- S.E.M.; *** $p < 0.001$, ** $p < 0.01$

892
893



894
895

896 **Fig. 3. Neural feature representations as a function of memory competition.** **a**, Anatomical ROIs
897 visualized on the Freesurfer average cortical surface. **b**, Color information as a function of memory
898 competition. Color information was defined as the fMRI pattern similarity between pairs of same-color
899 objects relative to pattern similarity between baseline pairs of objects (see **Fig. 1b**). Color information was
900 significantly stronger in the competitive than non-competitive condition (i.e., values greater than 0) across
901 the set of ROIs as a whole and in LO and vIPS individually (p 's < .05). **c**, Pairmate similarity as a function
902 of memory competition. Pairmate similarity was defined as the fMRI pattern similarity between pairmate
903 objects relative to pattern similarity between baseline pairs of objects. Only vIPS showed significantly
904 greater pairmate similarity in the competitive than non-competitive conditions (p = 0.004). Error bars reflect
905 \pm S.E.M.; ** p < 0.01, * p < 0.05

906

907

908
909

910 **Fig. 4. Neural measures of pairmate (dis)similarity predict color memory bias in vIPS. a**, Mean
911 correlation between vIPS pairmate dissimilarity during recall and mean signed color memory distance.
912 Correlations were performed within participant and correlation coefficients were *z*-transformed. For the
913 competitive condition, the mean correlation was significantly positive ($p = 0.004$), indicating that greater
914 pairmate dissimilarity in vIPS was associated with a stronger bias to remember pairmates' colors as away
915 from each other. There was no correlation between vIPS pairmate dissimilarity and signed color memory
916 distance for the non-competitive condition ($p = 0.566$). **b**, Relationship between vIPS pairmate dissimilarity
917 (binned into low, medium, high groups) and mean signed color memory distance (purple) and associative
918 memory accuracy (teal). Mean signed color memory distance and associative memory accuracy each
919 significantly varied as a function of vIPS dissimilarity (p 's $< .05$), with greater vIPS dissimilarity associated
920 with greater mean signed color memory distance and higher associative memory accuracy. *** $p < 0.001$,
921 * $p < 0.05$

